Stereotactic and Functional Neurosurgery

Stereotact Funct Neurosurg , DOI: 10.1159/000546716
Received: March 6, 2025
Accepted: May 22, 2025
Published online: June 18, 2025

Structural connectivity of the basal ganglia from patient-individual tractography is key for understanding the effects of deep brain stimulation in Parkinson's Disease

Loução R, Kocher M, Brandt GA, Petry-Schmelzer JN, Barbe M, Dafsari H, Mana J, Jech R, Wirths J, Visser-Vandewalle V, Andrade P, Baqapuri H, Luehrs M, Linden DEJ, Santyr B, Lozano A, Bongioanni A, Jarraya B, Cukur T

ISSN: 1011-6125 (Print), eISSN: 1423-0372 (Online)
https://www.karger.com/SFN
Stereotactic and Functional Neurosurgery

Research Article

Structural connectivity of the basal ganglia from patient-individual tractography is key for understanding the effects of deep brain stimulation in Parkinson's Disease

Ricardo Loução[a,b], Martin Kocher[a], Gregor Alexander Brandt[c], Jan Niklas Petry-Schmelzer[c], Michael Barbe[c], Haidar Dafsari[c], Josef Mana[d], Robert Jech[d], Jochen Wirths[a], Veerle Visser-Vandewalle[a], Pablo Andrade[a]

and the NEURIPIDES Study Group: Halim Baqapuri[e], Michael Luehrs[f,g], David E. J. Linden[e], Brendan Santyr[h], Andres Lozano[h], Alessandro Bongioanni[i], Bechir Jarraya[i,j], Tolga Cukur[k]

[a] Department of Stereotactic and Functional Neurosurgery, Faculty of Medicine and University Hospital Cologne, University of Cologne, Cologne, Germany
[b] Department of General Neurosurgery, Faculty of Medicine and University Hospital Cologne, University of Cologne, Cologne, Germany
[c] Department of Neurology, Faculty of Medicine and University Hospital Cologne, University of Cologne, Cologne, Germany
[d] Department of Neurology and Centre of Clinical Neuroscience, First Faculty of Medicine, Charles University, Prague, Czech Republic
[e] Mental Health and Neuroscience Research Institute, Maastricht University Medical Centre, Maastricht, The Netherlands
[f] Department of Cognitive Neuroscience, Faculty of Psychology and Neuroscience, Maastricht University, The Netherlands
[g] Research Department, Brain Innovation BV, Maastricht, The Netherlands
[h] Division of Neurosurgery, Department of Surgery, Toronto Western Hospital, University of Toronto, Toronto, Ontario, Canada
[i] Cognitive Neuroimaging Unit, CEA, INSERM, Université Paris-Saclay, NeuroSpin Center, 91191, Gif/Yvette, France
[j] Movement Disorders Unit, Foch Hospital, Université Paris-Saclay (UVSQ), Suresnes, France
[k] Department of Electrical and Electronics Engineering, National Magnetic Resonance Research Center (UMRAM), Bilkent University, Ankara 06800, Turkey

Short Title: Structural Connectivity in DBS for Parkinson
Corresponding Author: Martin Kocher
E-mail address: martin.kocher@uk-koeln.de

Keywords: Parkinson's disease, deep brain stimulation, tractography, structural connectivity

Abstract

Introduction: In Parkinson's disease (PD) patients, modulation of the fibre tracts of the cortico-basal ganglia-thalamo-cortical loop is the presumed mechanism of action of deep brain stimulation (DBS) of the subthalamic nucleus (STN). Therefore, we explored patient-individual cortical structural connectivity of the volume of tissue activated (VTA), as well as DBS-induced modulation of fibre tracts connecting the STN with cortical and subcortical nodes, and their correlation with therapeutic effects.

Methods: A retrospective cohort of n = 69 PD patients treated with bilateral DBS of the STN was analysed. Clinical response was assessed from the DBS-induced change in the UPDRS-III motor scores (total and symptom-specific sub-scores) under regular medication after a median follow-up of 9.0 (range 2.6 – 20.2) months. Tractography based on patient-individual diffusion-weighted MRI was employed in two ways. Whole brain tractography was used to identify the cortical connections of fibres passing the VTAs, and reconstruction of specific white matter pathways of the motor loop connecting the STN with the basal ganglia and cortex were used to identify the proportion of fibres within these pathways which was modulated by STN-DBS. This proportion of pathway modulation was used in a correlative analysis with clinical outcomes.

Results: Fibres traversing the VTAs were primarily connected to the supplementary motor area (SMA) and to a lesser degree to the premotor cortex. Within the pathways connecting the STN with the cortical and subcortical nodes, on average 30-40% (range 10-80%) of the fibres were modulated by STN-DBS. This proportion correlated significantly with the percentage change in UPDRS motor score for fibres connecting the STN with the SMA (ρ=0.28), pre-SMA (ρ=0.26), ventral and dorsal pre-motor cortices (ρ=0.26 and ρ=0.29, respectively), and the globus pallidus externus (GPe, ρ=0.26) and internus (GPi, ρ=0.29). Also, good clinical responses for both tremor and rigidity were associated with a significantly ($p < 0.05$) higher proportion of modulated fibres for the same cortico- and sub-cortico-STN connections.
Conclusion: Patient-individual tractography reveals that, in PD, most of the cortical fibres traversing the VTA are connected to the SMA. In addition, clinical efficacy is related to the proportion of DBS-affected fibres connecting the STN with nodes of both the hyperdirect (cortex-STN) and the indirect pathways (STN-basal ganglia). As such, patient-specific tractography, in particular in the basal ganglia, could be used in a clinical context as a tool to guide therapy.

Introduction

Everyday voluntary movements are the result of a well-orchestrated and balanced activity of a large number of skeletal muscles, which are initiated and executed almost effortlessly. It is assumed that the desired sequences of muscle activations are generated by temporally and spatially organised neuronal activity within the cortico-basal ganglia–thalamo-cortical motor loop [1], see Figure 1. According to a provisional model of movement and action control [2-4], an intended motor action first leads to fast, excitatory input from the cortex to the subthalamic nucleus (STN) via the hyperdirect pathway (HDP), resulting in broad inhibition of unnecessary or interfering movements by activation of the globus pallidus internus/substantia nigra pars reticularis (GPi/SNr), which in turn inhibits the thalamus and cortex. An appropriate motor program is then selected by activation of the striatum (STR), subsequent inhibition of the GPi/SNr via the direct pathway and release/disinhibition of the desired activity in the thalamus and cortex. This program is antagonised and/or terminated via the indirect pathway, which connects the STR to the GPi/SNr via the globus pallidus externus (GPe) and the STN.

In Parkinson's disease (PD), loss of dopaminergic neurons in the substantia nigra pars compacta (SNc) leads to changes in the excitability of neurons in the putamen (PUT), a part of the STR, which results in pronounced motor symptoms including akinesia/bradykinesia, rigidity, and tremor. Loss of dopamine in the striatum reduces the excitability of the direct pathway and increases the excitability of the indirect pathway, rendering the STN and GPi/SNr hyperactive and inducing pathological low-beta-band oscillatory synchrony of the basal ganglia and motor cortex, which is associated with the motor symptoms [5].

Deep brain stimulation (DBS) of the STN is an established therapy for patients with advanced PD who do not respond to drug treatment. Despite its well-documented efficacy, the exact mechanism of STN-DBS is only partially understood. The classical view is that high-frequency DBS suppresses local pathological STN activity and, as such, represents a reversible type of lesion [6]. However, DBS also induces remote effects such as ortho- and antidromic generation and propagation of action potentials, as well as affection of local synaptic transmission of pathways afferent to the site of stimulation, and may, as such, interfere with the pathological neural activity at various sites [7-9]. These network-level effects seem to play an important role in the mechanism of action of DBS, and increasingly more work is now focusing on identifying the fibre tracts that connect the above-mentioned cortical and subcortical structures and how these can be targeted by DBS [10, 11]. This connectomic approach is also based on the realisation that the STN has a three-part structure in which parts connected to the motor, associative, and limbic loops are in close proximity [12-14]. In addition, the supplementary motor area (SMA) seems to have a strong connection with the motor part of the STN via the HDP, which could represent a main target for DBS [15].

In several previously published reports, normative connectomes were used where average fibre tracts are constructed in standard brain templates and analysed in combination with patient-specific volumes of tissue activated (VTA) by DBS [16-24]. Although this approach has led to valuable insights, it remains unclear to what extent the normative connectomes can represent the actual structural connectivity of individual, mostly elderly patients. In the present study, we therefore performed state-of-the-art patient-specific tractography from preoperative diffusion-weighted MR imaging (DWI) in patients that received STN-DBS for PD. We first applied a whole-brain tractography reconstruction approach where we determined the specific cortical areas whose connections are modulated by STN-DBS by isolating the streamlines passing through the VTAs. To investigate correlations between clinical outcome and modulation of specific pathways, we used a second tracking approach where, based on the results of the first approach, we reconstructed the relevant pathways of the cortico-basal ganglia-thalamo-cortical loop for each patient and then computed the fraction of fibres within these tracts that were modulated by the VTAs. We hypothesised that these measures represent the magnitude of the modulatory effect in the different tracts of the motor loop and allow to identify the fibre tracts whose modulation correlates with motor outcomes as defined in the Unified Parkinson's Disease Rating Scale, part III (UPDRS-III), scoring system.

Patients and methods

Patients and clinical response assessment

This retrospective study included 69 patients (23 female) with a median age of 63.7 (range 46.8 – 78.1) years with PD (Hoehn-Yahr stages 1 to 4; average disease duration 10.4, range 2.6 – 27.2 years, Table 1) who were treated with bilateral DBS of the STN at the University Hospital Cologne from 2016 – 2021 and received longitudinal neurological evaluation including UPDRS scores by the treating neurologists. DBS surgery was performed under guidance of MR imaging fused with a stereotactic CT scan, as well as intraoperative electrophysiological and/or neurological monitoring. Clinical response was assessed from the DBS-induced change in the total UPDRS-III motor scores under regular medication (Med ON) after an average interval of 9.0 (range 2.6 – 20.2) months, at which point the stimulation settings were taken for VTA calculation. In addition, pre- and postoperative sum scores for individual symptoms (tremor, rigidity, and bradykinesia) were extracted from the UPDRS-III score sheets. Pre- and postoperative medication were transformed into the levodopa-equivalent dose (LEDD) [25]. The study was approved by the local ethics committee (No. 21-117).

Imaging procedures

Preoperatively, patients underwent an MRI scanning battery (Philips 3T Ingenia Elition, Eindhoven, The Netherlands), which included structural T1-weighted (165 slices; TR = 9.7 ms; TE = 4.8 ms; flip angle = 8°; voxel size = 0.5x0.5x1 mm^3) and T2-weighted (80 slices; TR = 3000 ms; TE = 80 ms; flip angle = 90°; voxel size = 0.5x0.5x2 mm^3), as well as diffusion-weighted images (DWI). The diffusion-weighted data were acquired using an echo-planar imaging (EPI) sequence (60 slices without slice gap; TR = 8141 ms; TE = 100 ms; 40 gradient directions with b-value 1000 s/mm^2; and a voxel size = 2×2×2 mm^3). Additional EPI images were acquired without diffusion weighting (b-values = 0 s/mm^2) and opposing phase-encoding directions for correction of susceptibility artefacts. One day postoperatively, patients underwent a CT scan to control the position of the DBS electrodes.

Pre-processing of the DWI data included noise reduction [26] and correction of eddy current artefacts using TORTOISE's (https://tortoise.nibib.nih.gov) [27, 28] *diffprep* routine. Susceptibility artefacts were corrected via *drbuddi* [29], using the T2-weighted image as a reference. Afterwards, field inhomogeneities were corrected using the routine *dwibiascorrect* of MRtrix3 (https://www.mrtrix.org) [30] with the *ants* algorithm [31], and finally the images were resampled to 1.3x1.3x1.3 mm^3 resolution according to the MRtrix recommendations.

MRtrix3 was also used to model the diffusion signal based on constrained spherical deconvolution (CSD) [32]. First, patient-specific tissue response functions were calculated using *dwi2response,* and study-specific tissue responses were obtained by averaging the patient-specific ones, using *responsemean*. These latter response functions were then used to calculate the patient-specific fibre orientation distributions (FOD) using *sst3_csd_beta1* from MRtrix3Tissue (https://3tissue.github.io), a fork of MRtrix3 which has been shown to be better suited for DWI data acquired with a single b-value [33]. Finally, the FOD data were normalised using *mtnormalise*.

Further image processing included the registration of T2-weighted images to the MNI 2009c non-linear asymmetric standard brain template [34] through a combination of linear and non-linear transformations, calculated using ANTs [35]. In addition, postoperative CTs were registered to the structural MRI data using linear transformations (ANTs) and VTAs were generated using the SimBio [36] and FieldTrip [37] suites, using the default settings available through LEAD-DBS (https://www.lead-dbs.org, v2.5.3) [38].

Tractography

We investigated two different fibre tracking approaches, both using MRtrix3 *tckgen* with the *ifod2* algorithm. First, we reconstructed a whole-brain tractogram using anatomically constrained tractography (ACT) [39], where 20 million tracts were generated by seeding from the white matter-grey matter interface generated using the T1-weighted image. The VTAs were then superimposed on the whole-brain tractogram and used to filter streamlines running through them. The number of

streamlines crossing the VTA and terminating in ipsilateral cortical regions, as defined in the fine-grained Glasser atlas [40], was identified for both hemispheres, averaged across hemispheres for each patient, and visualised in FreeSurfer (https://surfer.nmr.mgh.harvard.edu).
Since the streamline counts obtained in the first approach cannot be readily pooled across patients – see Discussion – , they are not suited for a correlation analysis with the clinical outcomes. Therefore, in a second approach, we generated tractograms of relevant pathways in the cortico-basal ganglia-thalamo-cortical loop – Figure 1 – and identified the proportion of modulated fibres for each pathway. Cortical regions-of-interest (ROI), as identified in the first approach – see Results – , included the primary motor (M1) area, the SMA, the pre-SMA, and the dorsal and ventral pre-motor areas (PMd and PMv, respectively), and were defined by the Human Motor Area Template (HMAT) [41]. Subcortical structures of interest included the putamen, the GPe, the GPi, the STN, and the thalamus as defined by the DISTAL atlas [42]. These structures were warped to the individual T2 images and then resliced to match the resolution of the diffusion-weighted images. Connections between pairs of nodes in this network were individually tracked for each patient, in which each voxel in the start ROI was seeded 2197 (13^3) times - an isotropic lattice with step size 0.1 mm, overlayed on the 1.3x1.3x1.3 mm^3 voxels. Streamlines were excluded if they entered any node in the network apart from those involved in the tracked pathway. The proportion of modulated fibres was calculated for each hemisphere by taking the ratio of affected streamlines (those overlapping with the VTA) to the total amount of reconstructed streamlines. These values were then averaged from both hemispheres and used to identify connections associated with an improvement in the total UPDRS-III score and in the symptom scores.

Statistical analysis
Clinical scores for the pre- and postoperative evaluations were compared via Wilcoxon's signed rank test. Since the total UPDRS-III score has a range between 0 to 108, it was regarded as a quasi-continuous variable despite being composed of ordinal items. The percentage change in UPDRS-III motor score was calculated by $\Delta UPDRS = 100*(UPDRS_{preop}-UPDRS_{postop})/UPDRS_{preop}$, resulting in positive values in patients with an improvement. This measure was then correlated to the proportion of fibres modulated by STN-DBS using Spearman correlation. The same approach was applied to LEDD, where $\Delta LEDD = 100*(LEDD_{preop}-LEDD_{postop})/LEDD_{preop}$.
In addition, pre- and postoperative scores for the symptoms tremor, rigidity, bradykinesia were computed by adding the respective single items from the UPDRS scale (tremor: items 20 and 21, 7 sub-items; rigidity: item 22, 5 sub-items; bradykinesia: items 23-26, 8 sub-items). Since these scores stem from a reduced number of ordinal items in the UPDRS-III scale, a different definition of clinical response was employed. A linear regression between the baseline and follow-up values was used to model the expected response, from which the postoperative effect of STN-DBS for each patient could be determined based on the preoperative values. Patients who fared better than the mean response as indicated by the regression line were categorised as "good responders" and those who did not were categorised as "bad responders", as demonstrated in Figure 2. The proportion of fibres modulated by the VTA in the different pathways and the $\Delta LEDD$ were then compared between these two groups with regard to the specific symptoms using Mann-Whitney U-test. False discovery rate correction was conducted using Benjamini-Hochberg's method, with an alpha value of 0.95.

Results
The clinical course of the patients after STN-DBS is summarised in Table 1. All clinical metrics were significantly reduced postoperatively. Of note, the average LEDD decreased from 1096.6 mg pre-operatively to 541.5 post-operatively ($p < 0.001$). Average VTA size was 54.0 µL, ranging from 2.2 to 305.4 µL.

Examples of whole brain VTA-filtered tractograms are shown in Figure 3, as well as the resulting cortical projections maps. The majority of the filtered streamlines were seeded in the SMA, followed

by the pre-SMA, PMd, and PMv. Some streamlines seeded in the M1 and S1 regions also traversed the VTAs, but to a much lesser extent.

Typical examples for the tractography within the structures of the cortico-basal ganglia-thalamo-cortical loop are depicted in Figure 4. The number of reconstructed streamlines from the STN to the GPe and GPi were orders of magnitude higher than those connecting with the cortex, shown in Figure 5. With regard to the HDP, the pre-motor regions had the most anatomical connections with the STN, followed by the primary motor and sensory cortices, and finally the pre-SMA and SMA. Only fibre tracts involving the STN were affected by the VTAs. The proportion of modulated fibres is shown in Figure 6, where the average proportion amounted to 36.0 +/- 16.7%, without any significant differences between the different pathways.

Regarding the clinical effects assessed by the total UPDRS-III score, a positive significant correlation between the degree of modulation and symptom improvement was found for almost all pathways involving the STN, except those to M1 and S1, as summarised in Table 2. The strongest correlations were seen for the fibre connections between the STN and GPi, the STN and PMd, as well as STN and SMA, whose scatterplots can be seen in Figure 7.

The distributions of the proportion of targeted fibres in the groups of good vs. bad responders as defined from the linear models for the UPDRS-III sub-scores are shown in Table 3. For rigidity, the good responders had a significantly higher proportion of fibres targeted for all tracts involving the STN (about 40% vs. 30%), and for tremor, this pattern was also seen except for connections STN-M1 and STN-S1. For bradykinesia, no significant differences in the proportion of modulated fibres between the groups was observed. Of note, no significant correlation between ?LEDD and ?UPDRS was found, and the ?LEDD in good responders did not significantly differ from that of the bad responders with respect to any of the sub-scores, see supplementary Tab. S1 .

Discussion

Main Findings

Preoperative patient-specific tractography was used to identify the fibre tracts associated with optimal DBS of the bilateral STN in a cohort of PD patients. The fibres traversing the VTA resulting from stimulation parameters at follow-up were predominantly connected to the ipsilateral SMA, as shown by the whole brain tractography reconstructions. Tractography of the cortico-basal ganglia-thalamo-cortical loop revealed that, on average, between 30-40% of the fibres connecting the STN with the cortical and subcortical regions of the motor loop were modulated by DBS. DBS-induced improvements of the UPDRS-III total score and sub-scores for tremor and rigidity correlated significantly with the VTA-modulated fraction of fibre connections between the STN and the pre-SMA, SMA, ventral/dorsal premotor cortex, as well as GPe and GPi.

Normative vs. patient-specific connectivity analyses

Many of the recent studies investigating the structural networks targeted by STN-DBS have applied normative connectomes in combination with patient-individual estimation of the VTAs DBS [16-24]. This procedure does not require the time-consuming acquisition of preoperative DWI data and can therefore be performed more easily in larger patient groups. However, it depends on the assumption that the average connectome of a cohort of healthy individuals or even PD patients from other remote centres is representative for an individual patient under investigation, at least in terms of general patterns of connectivity between the structures involved. As shown in Table 4, most of these analyses compared symptom scores 6-24 months after DBS to the preoperative situation, both under current medication (Med ON) or after withdrawal of medication (Med OFF). Quite consistently, these studies indicate that the improvement in overall UPDRS-III motor scores is associated with the

targeting of fibres projecting to the (ipsilateral) SMA and M1, while targeting projections to other frontal and prefrontal structures were less often found to be predictive.
In contrast, patient-specific connectomes were usually studied in smaller cohorts of 15-25 patients with shorter follow-up times and more variable outcome measures [43-48, 17, 49-51] , Table 5. As with normative connectomes, most of the studies found that modulating the connection between the STN and SMA and M1 was associated with clinical improvements. As such, the general view that DBS targeting the fibres between the STN and SMA or M1 is of clinical benefit seems to be supported by both types of analyses. Furthermore, in a direct comparison between patient-specific connectomes, group connectomes from PD patients, and normative connectomes of healthy subjects, Wang et al. [17] observed a high degree of agreement between brain connectivity profiles of the clinical STN-VTAs. However, the pattern of cortical STN connections that were correlated with a favourable outcome differed substantially between the three types of connectomes, probably due to a greater variance in the patient-specific connectomes. The present study found a significant correlation between clinical benefit and SMA-STN pathway modulation, further confirming its role in the STN-DBS therapy. However, no significant correlation was found between clinical outcome and M1-STN pathway modulation, contradicting some of the literature, possibly due to variability in connectome approaches.
We here applied a high-angular resolution diffusion-weighted imaging (HARDI) method that has major advantages compared to the more standard diffusion tensor imaging (DTI) often used in clinical practice. By using 40 diffusion directions, it allows to determine the fibre orientations with reasonable resolution and to account for crossing fibres. The associated tractography method is based on a model applying so-called constrained spherical deconvolution (CSD) [32] that delivers a fibre orientation distribution (FOD) function in every voxel, which can accommodate multiple fibre populations. Coupled with probabilistic tractography, this pipeline is much more sensitive to complex fibre arrangements and, therefore, suited for this kind of analysis. Still, it can be applied in the clinical setting where it takes about 10 min to acquire the MR images.
It is important to note, however, that the studies which employ patient-specific connectomes rely on the number of streamlines as a measure of connectivity between the VTA and specific target regions. The underlying assumption in such cases is that tractography-generated streamlines correlate with the number of axons which connect two nodes of interest, e.g. SMA and VTA. However, it is a well-known limitation of tractography that this is not the case: MR acquisition parameters, image quality, processing pipeline, pathway length, and underlying microstructure will all heavily influence the number of reconstructed streamlines, therefore confounding the analysis [52, 53]. A concrete example of such biases is shown in Figure 5, where shorter pathways (STN-GPe/GPi) resulted in many more streamlines than longer pathways (STN-Cortex). Part of the elegance of normative connectome analyses is that these avoid such confounding factors by making use of a predefined set of streamlines for the whole cohort, from which statistics are then drawn. In this work we stepped away from using raw streamline counts at the patient level, opting instead for tracking specific pathways of interest and investigating the degree of modulation in each individual hemisphere. In a way, this approach is similar to application of a normative connectome, in that statistics are drawn from a set of common streamlines: whole tract and modulated tract share the same streamline set, with the difference being that we generate these common streamline sets for each patient. While the aforementioned confounds might not be fully resolved with the proposed approach, we believe this method is more reflective of the DBS effects than simply counting the number of streamlines emanating from the VTA.

Efficacy of DBS targeting STN-cortical and STN-subcortical connections
The high level of connectivity consistently observed between the VTAs and the SMA and premotor cortex suggests that the clinically useful VTAs in PD preferentially target fibre tracts of the HDP. As indicated by several studies in non-human primates [54] and humans [14, 55 , 56-58], the HDP connects the primary motor cortex, SMA, and premotor cortex with the motor part of the STN and thus constitutes a significant part of the motor loop in the tripartite model of cortico-basal ganglia-

thalamo-cortical circuits [1, 59]. Of note, both experimental [54] and clinical [60] studies have identified separable clusters of the motor STN connected to the primary motor cortex and the SMA, each of which follows a somatotopic organization. DBS targeting of fibres connected to different clusters of the motor STN could therefore have differential effects on the motor symptoms of PD. The results from the connectivity studies shown in Tables 4 and 5 suggest that tremor is attenuated by modulating fibre connections between the STN with the primary motor cortex, while bradykinesia and rigidity are improved by stimulation of the SMA-STN or pre-SMA-STN fibre tracts [45, 24]. In the present study, we found that the clinical response of tremor and rigidity was associated with significantly higher fibre targeting not only between STN and pre-SMA/SMA, but also between STN and premotor cortex and STN and sensorimotor cortex, suggesting that modulation of a network rather than a single node contributes to the clinical efficacy of STN-DBS. Comparable observations have been made with MR guided high-focused ultrasound subthalamotomy, where distinct clusters corresponding to symptom improvements were identified within the motor STN [61]. The tremor-effective cluster corresponded to the part of the motor STN connected with the sensorimotor cortex, the bradykinesia-effective cluster fitted best with the SMA-connected cluster while the rigidity-effective cluster was located in between [61].

Apart from the HDP, the VTAs from STN-DBS usually also overlap with fibre tracts connecting the STN with the subcortical structures and, therefore, potentially modulate neural activity in the indirect pathway. Due to the dense arrangement and the complex fibre architecture, tractography of the basal ganglia nuclei and thalamus is more difficult and less reliable and has therefore been predominantly performed in publicly available high-quality diffusion MR data sets [62, 63, 42, 56, 64]. Hollunder et al. [23], by application of a normative connectome in conjunction with the Basal Ganglia Atlas [56], found that UPDRS-III improvement was associated with DBS targeting the fibres connecting the GPe with the premotor STN territory. In the present study, we also observed that STN-DBS targeted fibres connecting the STN with the GPe and GPi to a substantial amount and that this contributed to the clinical efficacy of the DBS.

In the present study, we calculated the proportion of fibre connections between two structures passing through the VTA as a measure of modulation strength. Although this approach may not seem obvious at first glance, it has been shown to be useful in both clinical and theoretical studies. In a recent paper by Segura-Amil et al. [51], the term ‘activation’ was applied to streamlines passing through a given VTA and it was shown that an activation of 50% of the HDP was required to achieve a clinical effect in PD patients. Kähkölä et al. [50] used patient-specific tractography to identify the cluster of the STN connected with the pre-SMA and found that only when this cluster was stimulated, i.e. more than 50% of the cluster covered by the VTA, did patients respond well to treatment in terms of unilateral motor improvement. Interestingly, in one of the most detailed large-scale simulation models of the cortico-basal ganglia network, a similar measure, i.e. DBS-induced percent fibre activation, was found to be a useful variable for predicting pathological thalamic activity [65], where the authors found that the optimal stimulation activated 88% of the HDP fibres, 56% of the STN-GPi fibres, and 46% of the STN-GPe fibres.

Relation between STN structural connectivity and neurophysiological effects of DBS

According to a recent comprehensive update on the neurophysiological mechanisms, DBS has both local and remote electrophysiological effects [9]. In the STN, DBS seems to mainly induce suppression of neural activity by activation of local GABA-ergic synapses, while the network effects are probably the result of antidromic propagation of action potentials along the long-range afferents. This view is supported by evidence from EEG, ECoG, MEG, and local field potential (LFP) recordings showing that STN-DBS stimulation not only suppresses pathologic synchronised beta activity in the basal ganglia, but also modulates cortical beta activity [66, 67]. In addition, STN-DBS reduces cortical pathologic beta-gamma cross-frequency coupling and high beta-band coherence between cortex and STN [15]. Of note, at least the latter effect seems to be confined to the part connected to the SMA [7] and, as such, points to the HDP as an important structure supporting the modulatory effect of STN-DBS. This view is further strengthened by a combined LFP-MEG analysis where the high-beta band SMA activity

was found to selectively drive STN activity by means of propagation along the HDP which depended on the fibre density of the HDP [15].
Recently, a new neurophysiological biomarker has been proposed that studied phase-amplitude coupling of the beta-band with high-frequency oscillations (HFO) in the STN, rather than looking at beta-power itself. Beta-HFO phase-amplitude coupling was specifically present in the motor STN, and the respective VTAs were structurally mainly connected to the SMA in contrast to the other contacts that influenced much wider frontal and parietal regions [68]. Together, these results confirm the hypothesis that modulation of activity of the HDP and especially the of the fibres connecting the SMA with the motor STN plays an important role for the clinical effect of STN-DBS.
In principle, activity in the HDP could also be modulated by direct stimulation of the motor cortex, which has indeed been evaluated in a limited number of patients not suitable for STN-DBS [69]. However, as argued by Cioni et al. [69], motor cortex stimulation is performed below the threshold for movements and presumably interferes with small inhibitory axons in the cortex and orthodromic or antidromic activation of fibres connecting the motor cortex to the basal ganglia, rather than acting on the pyramidal cells. It may as such decrease cortical excitability or disrupt oscillatory rhythms and abnormal patterns of activity, and seems to have some positive long-term effects mainly on axial symptoms.

Limitations
The data of the present study originate from patients who were examined at different time intervals after implantation of the DBS electrodes. After STN-DBS surgery, lesion effects can take some months to wane and patients often experiment multiple stimulation settings until an optimal programme is found. Our cohort thus potentially included patients with clinically sub-optimal settings. On the other hand, DBS effects may also wane over time and even with perfectly implanted electrodes, effects might not be seen at long follow-up times. It is, however, worth noting that including sub-optimal stimulation parameters can be of statistical benefit, as it reduces selection bias and helps reveal the true underlying effect. Although we aimed to identify the main individual structural connections within the basal ganglia, the present tractography method is probably still too crude to resolve the dense arrangement and complex architecture of curved and collateralized fibre tracts within the Forel field. These fibres connect, among others, the GPi and STN to the thalamic subnuclei, run in close proximity to the zona incerta and have also been shown to be effective targets in DBS for PD [70-73].
Our cohort was also evaluated in the “on medication” state. Clinical outcomes evaluated here are thus potentially an effect of both medication and STN-DBS, and these cannot be truly separated. However, as indicated in a separate analysis, clinical response was not significantly correlated with the reduction of LEDD, supporting the view that the reduced need for medication represents an additional effect of DBS. Additionally, the UPDRS-III scores, which reflect only motor symptoms, are a single domain of affliction of PD patients. Patients with PD are often also afflicted by non-motor symptoms, which were not evaluated here. A more comprehensive, multi-centre analysis is already planned, where all these effects will be taken into consideration to better characterise the relation between STN-DBS and overall clinical outcome.

Conclusion
Patient-individual tractography reveals that, in PD, most of the cortical fibres that run through the VTA connect to the SMA. In addition, clinical efficacy is related to the proportion of DBS-modulated fibres connecting the STN with nodes of both the HDP and the indirect pathway. As such, patient-specific tractography, in particular in the basal ganglia, could be used in a clinical context as a tool to guide surgical therapy.

Acknowledgements
We would like to thank E. Güngör for her support with data collection.

Statement of Ethics

This study protocol was reviewed and approved by the ethics committee of the Medical Faculty of the University of Cologne, approval number 21-1117. All patients gave their informed written consent for the treatment with deep brain stimulation. Due to the retrospective character of the study, the ethics committee granted an exemption from requiring written informed consent for the analysis of clinical and imaging data.

Conflict of interest statement

Andres M. Lozano: Consultant for Medtronic, Boston Scientific, Abbott, Insightec and Functional Neuromodulation; Veerle Visser-Vandewalle and Andres M. Lozano were both a member of the journal's Editorial Board at the time of submission. All other authors have no conflicts of interest to declare.

Funding Sources

Funds have been provided by the European Joint Programme Neurodegenerative Disease Research (JPND) 2020 call "Novel imaging and brain stimulation methods and technologies related to Neurodegenerative Diseases" for the Neuripides project 'Neurofeedback for self-stImulation of the brain as therapy for ParkInson Disease'. The Neuripides project has received funding from the following funding organizations under the aegis of JPND: The Netherlands, The Netherlands Organization for Health Research and Development (ZonMw); Germany, Federal Ministry of Education and Research (BMBF); Czech Republic, Ministry of Education, Youth and Sports (MEYS); France, French National Research Agency (ANR); Canada, Canadian Institutes of Health Research (CIHR); Turkey, Scientific and Technological Research Council of Turkey (TUBITAK).

Author Contributions

RL – Conceptualisation, methodology, formal analysis, writing of original draft, manuscript review and editing. MK – Conceptualisation, methodology, writing of original draft, manuscript review and editing. GB – Resources, data curation, manuscript review and editing. JP-S – Resources, data curation, manuscript review and editing. MB – Resources, data curation, manuscript review and editing. HD – Resources, data curation, manuscript review and editing. JM – Methodology, manuscript review and editing. RJ – Methodology, manuscript review and editing. JW – Resources, data curation, manuscript review and editing. VVV – Supervision, conceptualisation, funding acquisition, manuscript review and editing. PA – Supervision, conceptualisation, manuscript review and editing. HB – Conceptualisation, manuscript review and editing. ML - Conceptualisation, manuscript review and editing. DEJ-L – Supervision, conceptualisation, manuscript review and editing. BS - Conceptualisation, manuscript review and editing. AL - Conceptualisation, manuscript review and editing. AB - Conceptualisation, manuscript review and editing. BJ - Conceptualisation, manuscript review and editing. TC - Conceptualisation, manuscript review and editing.

Data Availability Statement

The individual clinical and imaging data supporting the results of this study are not publicly available as they contain information that could compromise patient privacy but aggregated and/or anonymised data are available upon reasonable request to the author RL.

References

1. Alexander GE, Crutcher MD, DeLong MR. Basal ganglia-thalamocortical circuits: parallel substrates for motor, oculomotor, "prefrontal" and "limbic" functions. Prog Brain Res. 1990;85:119-46.
2. Mink JW. The basal ganglia: focused selection and inhibition of competing motor programs. Prog Neurobiol. 1996 Nov;50(4):381-425.
3. Nambu A, Tokuno H, Takada M. Functional significance of the cortico-subthalamo-pallidal 'hyperdirect' pathway. Neurosci Res. 2002 Jun;43(2):111-7.
4. Bonnevie T, Zaghloul KA. The Subthalamic Nucleus: Unravelling New Roles and Mechanisms in the Control of Action. Neuroscientist. 2019 Feb;25(1):48-64.
5. Obeso JA, Marin C, Rodriguez-Oroz C, Blesa J, Benitez-Temino B, Mena-Segovia J, et al. The basal ganglia in Parkinson's disease: current concepts and unexplained observations. Ann Neurol. 2008 Dec;64 Suppl 2:S30-46.
6. Ng PR, Bush A, Vissani M, McIntyre CC, Richardson RM. Biophysical Principles and Computational Modeling of Deep Brain Stimulation. Neuromodulation. 2024 Apr;27(3):422-39.
7. Oswal A, Beudel M, Zrinzo L, Limousin P, Hariz M, Foltynie T, et al. Deep brain stimulation modulates synchrony within spatially and spectrally distinct resting state networks in Parkinson's disease. Brain. 2016 May;139(Pt 5):1482-96.
8. Lozano AM, Lipsman N, Bergman H, Brown P, Chabardes S, Chang JW, et al. Deep brain stimulation: current challenges and future directions. Nat Rev Neurol. 2019 Mar;15(3):148-60.
9. Neumann WJ, Steiner LA, Milosevic L. Neurophysiological mechanisms of deep brain stimulation across spatiotemporal resolutions. Brain. 2023 Nov 2;146(11):4456-68.
10. Wong JK, Middlebrooks EH, Grewal SS, Almeida L, Hess CW, Okun MS. A Comprehensive Review of Brain Connectomics and Imaging to Improve Deep Brain Stimulation Outcomes. Mov Disord. 2020 May;35(5):741-51.
11. Andrews L, Keller SS, Osman-Farah J, Macerollo A. A structural magnetic resonance imaging review of clinical motor outcomes from deep brain stimulation in movement disorders. Brain Commun. 2023;5(3):fcad171.
12. Temel Y, Blokland A, Steinbusch HW, Visser-Vandewalle V. The functional role of the subthalamic nucleus in cognitive and limbic circuits. Prog Neurobiol. 2005 Aug;76(6):393-413.
13. Temel Y, Kessels A, Tan S, Topdag A, Boon P, Visser-Vandewalle V. Behavioural changes after bilateral subthalamic stimulation in advanced Parkinson disease: a systematic review. Parkinsonism Relat Disord. 2006 Jun;12(5):265-72.
14. Brunenberg EJ, Moeskops P, Backes WH, Pollo C, Cammoun L, Vilanova A, et al. Structural and resting state functional connectivity of the subthalamic nucleus: identification of motor STN parts and the hyperdirect pathway. PLoS One. 2012;7(6):e39061.
15. Oswal A, Cao C, Yeh CH, Neumann WJ, Gratwicke J, Akram H, et al. Neural signatures of hyperdirect pathway activity in Parkinson's disease. Nat Commun. 2021 Aug 31;12(1):5185.
16. Horn A, Reich M, Vorwerk J, Li N, Wenzel G, Fang Q, et al. Connectivity Predicts deep brain stimulation outcome in Parkinson disease. Ann Neurol. 2017 Jul;82(1):67-78.
17. Wang Q, Akram H, Muthuraman M, Gonzalez-Escamilla G, Sheth SA, Oxenford S, et al. Normative vs. patient-specific brain connectivity in deep brain stimulation. Neuroimage. 2021 Jan 1;224:117307.
18. Chen Y, Zhu G, Liu D, Liu Y, Zhang X, Du T, et al. Seed-Based Connectivity Prediction of Initial Outcome of Subthalamic Nuclei Deep Brain Stimulation. Neurotherapeutics. 2022 Mar;19(2):608-15.
19. Strelow JN, Baldermann JC, Dembek TA, Jergas H, Petry-Schmelzer JN, Schott F, et al. Structural Connectivity of Subthalamic Nucleus Stimulation for Improving Freezing of Gait. J Parkinsons Dis. 2022;12(4):1251-67.
20. Fan H, Guo Z, Jiang Y, Xue T, Yin Z, Xie H, et al. Optimal subthalamic stimulation sites and related networks for freezing of gait in Parkinson's disease. Brain Commun. 2023;5(5):fcad238.
21. Gadot R, Vanegas Arroyave N, Dang H, Anand A, Najera RA, Taneff LY, et al. Association of clinical outcomes and connectivity in awake versus asleep deep brain stimulation for Parkinson disease. J Neurosurg. 2023 Apr 1;138(4):1016-27.
22. Hacker ML, Rajamani N, Neudorfer C, Hollunder B, Oxenford S, Li N, et al. Connectivity Profile for Subthalamic Nucleus Deep Brain Stimulation in Early Stage Parkinson Disease. Ann Neurol. 2023 Aug;94(2):271-84.
23. Hollunder B, Ostrem JL, Sahin IA, Rajamani N, Oxenford S, Butenko K, et al. Mapping dysfunctional circuits in the frontal cortex using deep brain stimulation. Nat Neurosci. 2024 Mar;27(3):573-86.

24. Rajamani N, Friedrich H, Butenko K, Dembek T, Lange F, Navratil P, et al. Deep brain stimulation of symptom-specific networks in Parkinson's disease. Nat Commun. 2024 May 31;15(1):4662.
25. Tomlinson CL, Stowe R, Patel S, Rick C, Gray R, Clarke CE. Systematic review of levodopa dose equivalency reporting in Parkinson's disease. Mov Disord. 2010 Nov 15;25(15):2649-53.
26. Veraart J, Novikov DS, Christiaens D, Ades-Aron B, Sijbers J, Fieremans E. Denoising of diffusion MRI using random matrix theory. Neuroimage. 2016 Nov 15;142:394-406.
27. Pierpaoli C, Walker L, Irfanoglu MO, Barnett A, Basser P, Chang LC, et al. TORTOISE: an integrated software package for processing of diffusion MRI data. ISMRM. 2010;abstract #1597(18th annual meeting).
28. Irfanoglu MO, Nayak A, Jenkins J, Pierpaoli C. TORTOISE v3 : Improvements and New Features of the NIH Diffusion MRI Processing Pipeline. ISMRM. 2021;25th annual meeting, :abstract #3540.
29. Irfanoglu MO, Modi P, Nayak A, Hutchinson EB, Sarlls J, Pierpaoli C. DR-BUDDI (Diffeomorphic Registration for Blip-Up blip-Down Diffusion Imaging) method for correcting echo planar imaging distortions. Neuroimage. 2015 Feb 1;106:284-99.
30. Tournier JD, Smith R, Raffelt D, Tabbara R, Dhollander T, Pietsch M, et al. MRtrix3: A fast, flexible and open software framework for medical image processing and visualisation. Neuroimage. 2019 Nov 15;202:116137.
31. Tustison NJ, Avants BB, Cook PA, Zheng Y, Egan A, Yushkevich PA, et al. N4ITK: improved N3 bias correction. IEEE Trans Med Imaging. 2010 Jun;29(6):1310-20.
32. Tournier JD, Calamante F, Connelly A. Robust determination of the fibre orientation distribution in diffusion MRI: non-negativity constrained super-resolved spherical deconvolution. Neuroimage. 2007 May 1;35(4):1459-72.
33. Dhollander T, Raffelt D, Connelly A. Unsupervised 3-tissue response function estimation from single-shell or multi-shell diffusion MR data without a co-registered T1 image. ISMRM Workshop on Breaking the Barriers of Diffusion MRI. 2016:5.
34. Fonov V, Evans AC, Botteron K, Almli CR, McKinstry RC, Collins DL, et al. Unbiased average age-appropriate atlases for pediatric studies. Neuroimage. 2011 Jan 1;54(1):313-27.
35. Avants BB, Epstein CL, Grossman M, Gee JC. Symmetric diffeomorphic image registration with cross-correlation: evaluating automated labeling of elderly and neurodegenerative brain. Med Image Anal. 2008 Feb;12(1):26-41.
36. Vorwerk J, Oostenveld R, Piastra MC, Magyari L, Wolters CH. The FieldTrip-SimBio pipeline for EEG forward solutions. Biomed Eng Online. 2018 Mar 27;17(1):37.
37. Oostenveld R, Fries P, Maris E, Schoffelen JM. FieldTrip: Open source software for advanced analysis of MEG, EEG, and invasive electrophysiological data. Comput Intell Neurosci. 2011;2011:156869.
38. Horn A, Li N, Dembek TA, Kappel A, Boulay C, Ewert S, et al. Lead-DBS v2: Towards a comprehensive pipeline for deep brain stimulation imaging. Neuroimage. 2019 Jan 1;184:293-316.
39. Smith RE, Tournier JD, Calamante F, Connelly A. Anatomically-constrained tractography: improved diffusion MRI streamlines tractography through effective use of anatomical information. Neuroimage. 2012 Sep;62(3):1924-38.
40. Glasser MF, Coalson TS, Robinson EC, Hacker CD, Harwell J, Yacoub E, et al. A multi-modal parcellation of human cerebral cortex. Nature. 2016 Aug 11;536(7615):171-78.
41. Mayka MA, Corcos DM, Leurgans SE, Vaillancourt DE. Three-dimensional locations and boundaries of motor and premotor cortices as defined by functional brain imaging: a meta-analysis. Neuroimage. 2006 Jul 15;31(4):1453-74.
42. Ewert S, Plettig P, Li N, Chakravarty MM, Collins DL, Herrington TM, et al. Toward defining deep brain stimulation targets in MNI space: A subcortical atlas based on multimodal MRI, histology and structural connectivity. Neuroimage. 2018 Apr 15;170:271-82.
43. Koirala N, Fleischer V, Granert O, Deuschl G, Muthuraman M, Groppa S. Network effects and pathways in Deep brain stimulation in Parkinson's disease. Annu Int Conf IEEE Eng Med Biol Soc. 2016 Aug;2016:5533-36.
44. Vanegas-Arroyave N, Lauro PM, Huang L, Hallett M, Horovitz SG, Zaghloul KA, et al. Tractography patterns of subthalamic nucleus deep brain stimulation. Brain. 2016 Apr;139(Pt 4):1200-10.
45. Akram H, Sotiropoulos SN, Jbabdi S, Georgiev D, Mahlknecht P, Hyam J, et al. Subthalamic deep brain stimulation sweet spots and hyperdirect cortical connectivity in Parkinson's disease. Neuroimage. 2017 Sep;158:332-45.

46. Avecillas-Chasin JM, Alonso-Frech F, Nombela C, Villanueva C, Barcia JA. Stimulation of the Tractography-Defined Subthalamic Nucleus Regions Correlates With Clinical Outcomes. Neurosurgery. 2019 Aug 1;85(2):E294-E303.
47. Krishna V, Sammartino F, Rabbani Q, Changizi B, Agrawal P, Deogaonkar M, et al. Connectivity-based selection of optimal deep brain stimulation contacts: A feasibility study. Ann Clin Transl Neurol. 2019 Jul;6(7):1142-50.
48. Vassal F, Dilly D, Boutet C, Bertholon F, Charier D, Pommier B. White matter tracts involved by deep brain stimulation of the subthalamic nucleus in Parkinson's disease: a connectivity study based on preoperative diffusion tensor imaging tractography. Br J Neurosurg. 2020 Apr;34(2):187-95.
49. Gonzalez-Escamilla G, Koirala N, Bange M, Glaser M, Pintea B, Dresel C, et al. Deciphering the Network Effects of Deep Brain Stimulation in Parkinson's Disease. Neurol Ther. 2022 Mar;11(1):265-82.
50. Kahkola J, Lahtinen M, Keinanen T, Katisko J. Stimulation of the Presupplementary Motor Area Cluster of the Subthalamic Nucleus Predicts More Consistent Clinical Outcomes. Neurosurgery. 2023 May 1;92(5):1058-65.
51. Segura-Amil A, Nowacki A, Debove I, Petermann K, Tinkhauser G, Krack P, et al. Programming of subthalamic nucleus deep brain stimulation with hyperdirect pathway and corticospinal tract-guided parameter suggestions. Hum Brain Mapp. 2023 Aug 15;44(12):4439-51.
52. Jones DK. Challenges and limitations of quantifying brain connectivity in vivo with diffusion MRI. Imaging Med. 2010;2(3):341-55.
53. Jones DK, Knosche TR, Turner R. White matter integrity, fiber count, and other fallacies: the do's and don'ts of diffusion MRI. Neuroimage. 2013 Jun;73:239-54.
54. Haynes WI, Haber SN. The organization of prefrontal-subthalamic inputs in primates provides an anatomical substrate for both functional specificity and integration: implications for Basal Ganglia models and deep brain stimulation. J Neurosci. 2013 Mar 13;33(11):4804-14.
55. Petersen MV, Lund TE, Sunde N, Frandsen J, Rosendal F, Juul N, et al. Probabilistic versus deterministic tractography for delineation of the cortico-subthalamic hyperdirect pathway in patients with Parkinson disease selected for deep brain stimulation. J Neurosurg. 2017 May;126(5):1657-68.
56. Petersen MV, Mlakar J, Haber SN, Parent M, Smith Y, Strick PL, et al. Holographic Reconstruction of Axonal Pathways in the Human Brain. Neuron. 2019 Dec 18;104(6):1056-64 e3.
57. Emmi A, Antonini A, Macchi V, Porzionato A, De Caro R. Anatomy and Connectivity of the Subthalamic Nucleus in Humans and Non-human Primates. Front Neuroanat. 2020;14:13.
58. Milardi D, Basile GA, Faskowitz J, Bertino S, Quartarone A, Anastasi GP, et al. Effects of diffusion signal modeling and segmentation approaches on subthalamic nucleus parcellation. Neuroimage. 2022 Apr 15;250:118959.
59. Obeso JA, Rodriguez-Oroz MC, Benitez-Temino B, Blesa FJ, Guridi J, Marin C, et al. Functional organization of the basal ganglia: therapeutic implications for Parkinson's disease. Mov Disord. 2008;23 Suppl 3:S548-59.
60. Plantinga BR, Temel Y, Duchin Y, Uludag K, Patriat R, Roebroeck A, et al. Individualized parcellation of the subthalamic nucleus in patients with Parkinson's disease with 7T MRI. Neuroimage. 2018 Mar;168:403-11.
61. Rodriguez-Rojas R, Pineda-Pardo JA, Manez-Miro J, Sanchez-Turel A, Martinez-Fernandez R, Del Alamo M, et al. Functional Topography of the Human Subthalamic Nucleus: Relevance for Subthalamotomy in Parkinson's Disease. Mov Disord. 2022 Feb;37(2):279-90.
62. Pujol S, Cabeen R, Sebille SB, Yelnik J, Francois C, Fernandez Vidal S, et al. In vivo Exploration of the Connectivity between the Subthalamic Nucleus and the Globus Pallidus in the Human Brain Using Multi-Fiber Tractography. Front Neuroanat. 2016;10:119.
63. Cousineau M, Jodoin PM, Morency FC, Rozanski V, Grand'Maison M, Bedell BJ, et al. A test-retest study on Parkinson's PPMI dataset yields statistically significant white matter fascicles. Neuroimage Clin. 2017;16:222-33.
64. Shim JH, Baek HM. White Matter Connectivity between Structures of the Basal Ganglia using 3T and 7T. Neuroscience. 2022 Feb 10;483:32-39.
65. Spiliotis K, Butenko K, Starke J, van Rienen U, Kohling R. Towards an optimised deep brain stimulation using a large-scale computational network and realistic volume conductor model. J Neural Eng. 2024 Jan 4;20(6).
66. Weiss D, Klotz R, Govindan RB, Scholten M, Naros G, Ramos-Murguialday A, et al. Subthalamic stimulation modulates cortical motor network activity and synchronization in Parkinson's disease. Brain. 2015 Mar;138(Pt 3):679-93.
67. Abbasi N, Fereshtehnejad SM, Zeighami Y, Larcher KM, Postuma RB, Dagher A. Predicting severity and prognosis in Parkinson's disease from brain microstructure and connectivity. Neuroimage Clin. 2020;25:102111.

68. Bockova M, Lamos M, Chrastina J, Daniel P, Kupcova S, Riha I, et al. Coupling between beta band and high frequency oscillations as a clinically useful biomarker for DBS. NPJ Parkinsons Dis. 2024 Feb 21;10(1):40.
69. Cioni B, Tufo T, Bentivoglio A, Trevisi G, Piano C. Motor cortex stimulation for movement disorders. J Neurosurg Sci. 2016 Jun;60(2):230-41.
70. Voges J, Volkmann J, Allert N, Lehrke R, Koulousakis A, Freund HJ, et al. Bilateral high-frequency stimulation in the subthalamic nucleus for the treatment of Parkinson disease: correlation of therapeutic effect with anatomical electrode position. J Neurosurg. 2002 Feb;96(2):269-79.
71. Plaha P, Ben-Shlomo Y, Patel NK, Gill SS. Stimulation of the caudal zona incerta is superior to stimulation of the subthalamic nucleus in improving contralateral parkinsonism. Brain. 2006 Jul;129(Pt 7):1732-47.
72. Pollo C, Vingerhoets F, Pralong E, Ghika J, Maeder P, Meuli R, et al. Localization of electrodes in the subthalamic nucleus on magnetic resonance imaging. J Neurosurg. 2007 Jan;106(1):36-44.
73. Neudorfer C, Maarouf M. Neuroanatomical background and functional considerations for stereotactic interventions in the H fields of Forel. Brain Struct Funct. 2018 Jan;223(1):17-30.

Figure legends

Fig. 1. Schematic of the functional neuroanatomy of the cortico–basal ganglia–thalamo–cortical motor loop. Some connections are omitted for the sake of simplicity.
Fig. 2. Scatter plot of pre- vs postoperative rigidity score. The black dashed line is the result of linear regression of the displayed points, showing the expected STN-DBS effect. Patients whose postoperative score is below the prediction line are considered good responders (blue circles), while patients whose score is above the predicted one are considered bad responders (red circles).
Fig. 3. Examples of patient-individual fibre density map of connections between the clinical VTA's and the cortex (left) and the mean fibre density of the cortical connections of the VTA's filtered from whole-brain tractography in the total cohort in template space (right). S1: Primary somatosensory cortex, M1: primary motor cortex, SMA: supplementary motor cortex, preSMA: pre-supplementary motor cortex, PMd: dorsal premotor cortex, PMv: ventral premotor cortex.
Fig. 4. Pathway reconstructions in a representative patient. On the left, the involved ROIs are shown. On the other panels, reconstructed streamlines in each pathway (blue: unaffected by DBS, red: modulated by DBS) are shown. ROIs: cortex – green (involved in hyperdirect pathway); putamen – orange; GPe – pink; GPi – blue; STN – cyan; Thalamus – purple; VTA – yellow.
Fig. 5. Streamline counts of structural connections between the STN and cortical regions and basal ganglia nodes
Fig. 6. Percentage of fibres modulated by STN-DBS for each pathway.
Fig. 7. Scatter plots of the proportion of fibres modulated by STN-DBS and the percentage improvement in UPDRS-III score for the most significantly correlated pathways

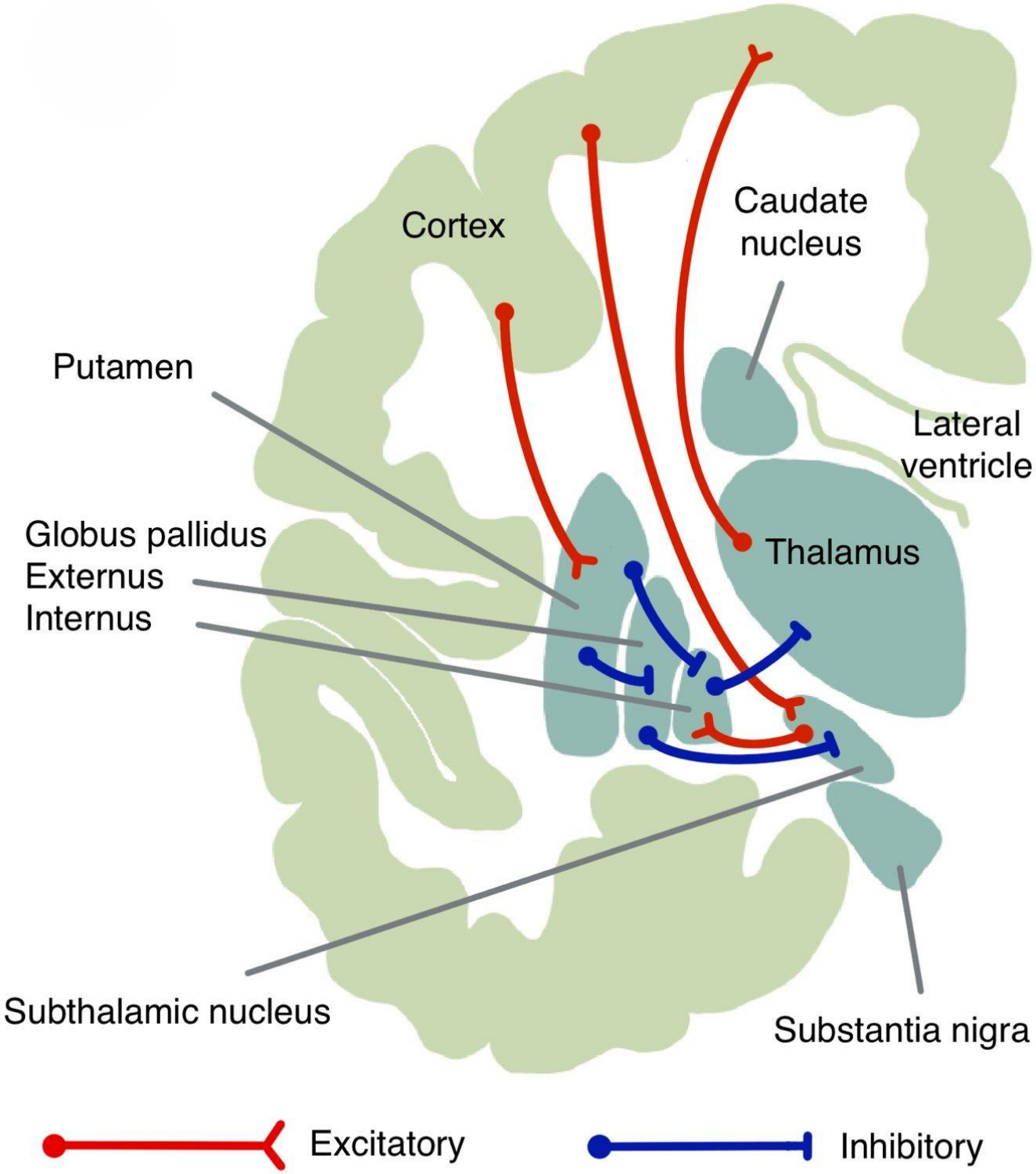

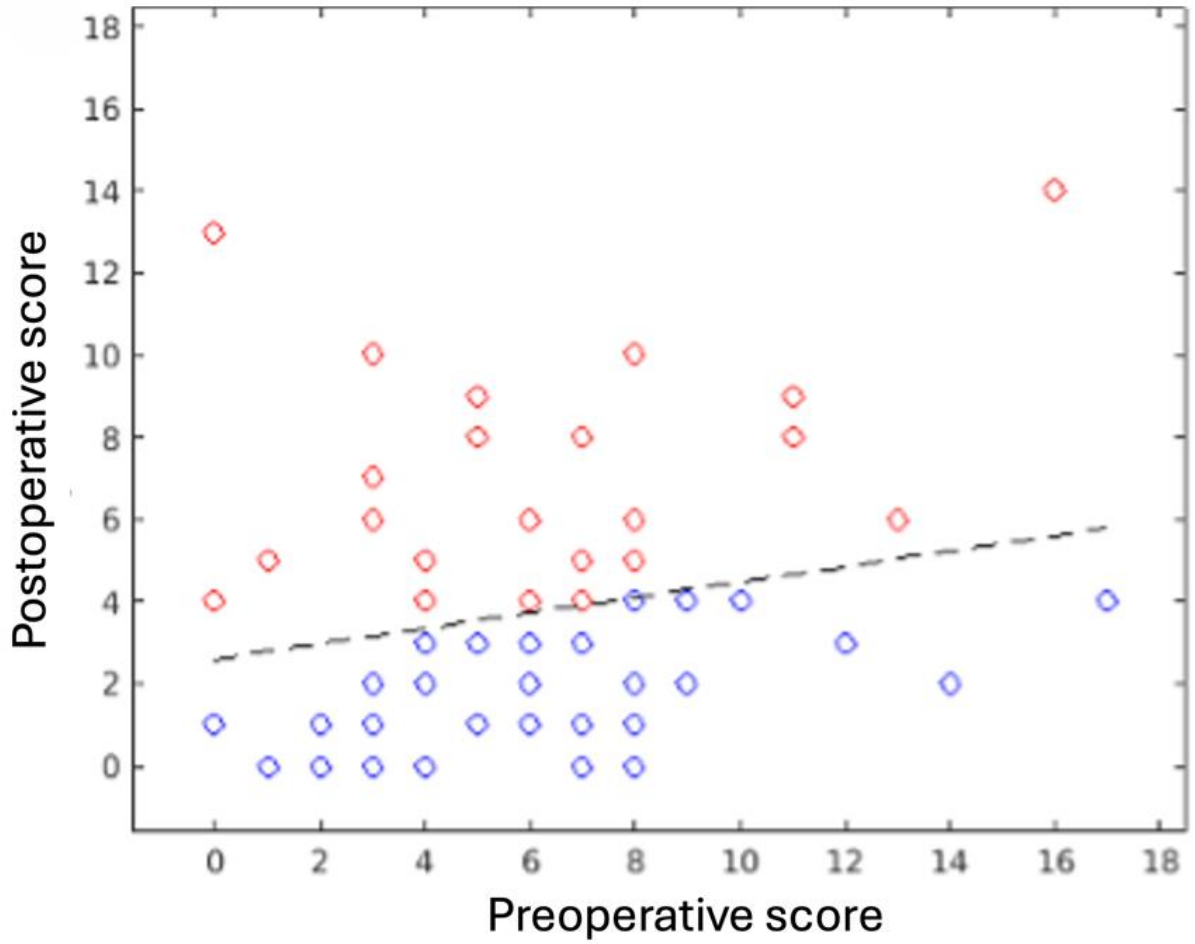

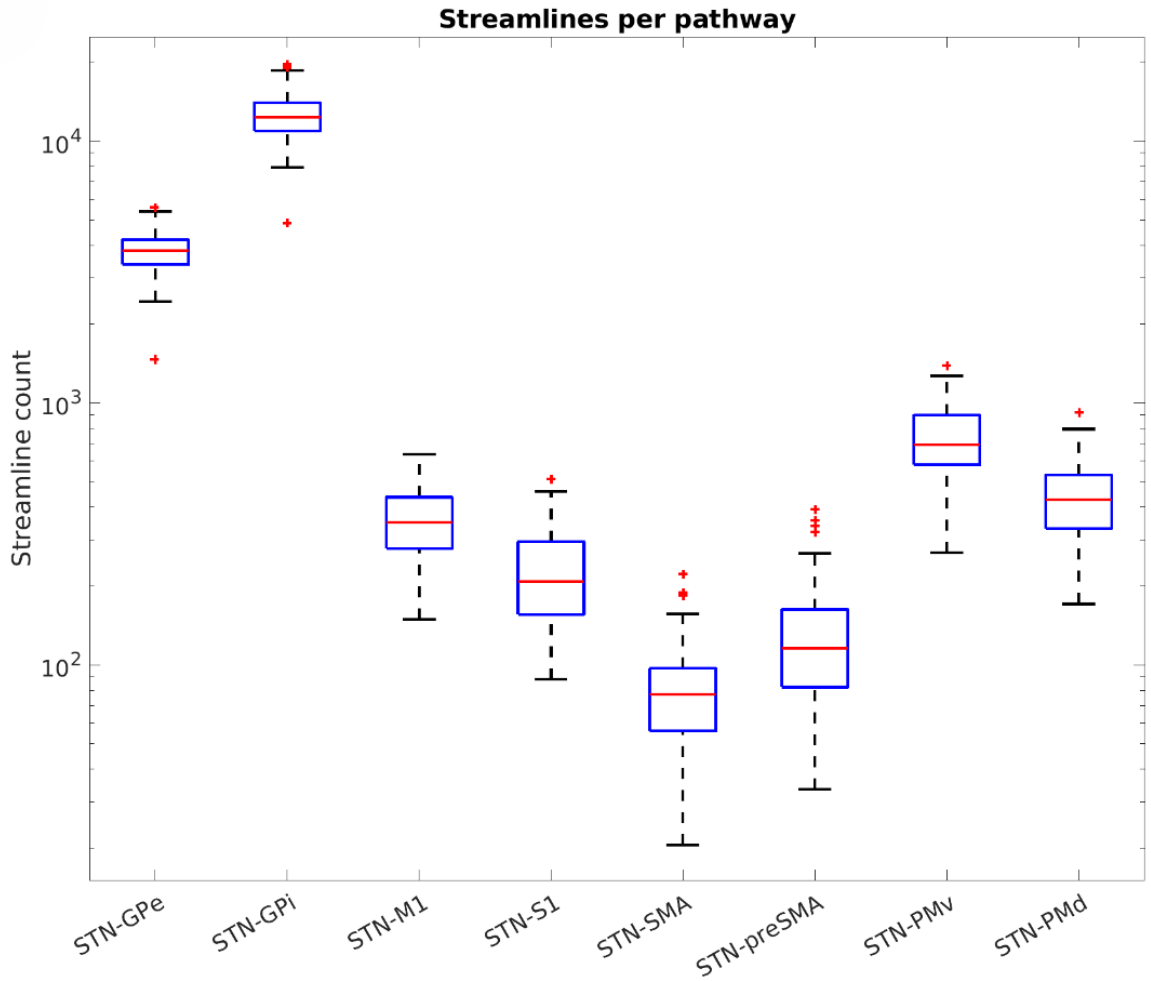

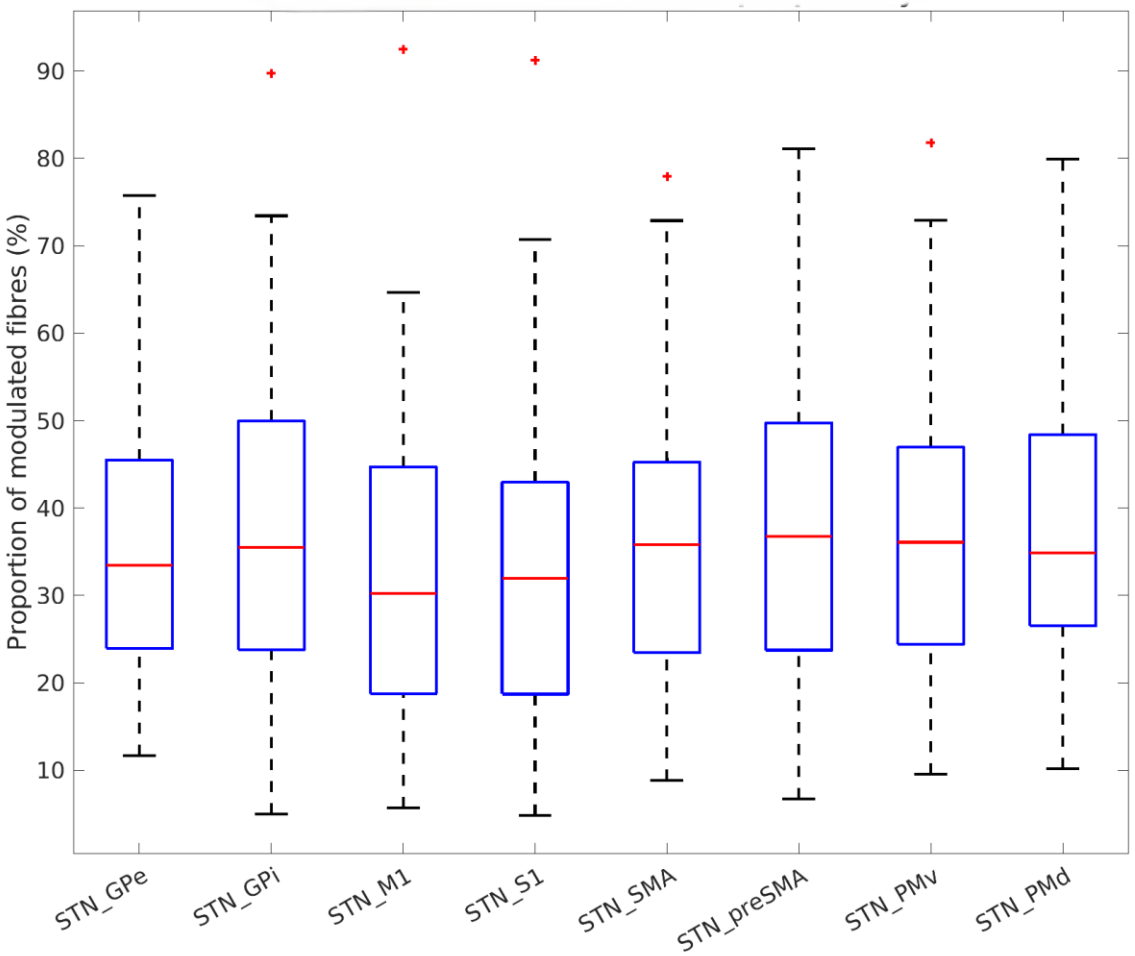

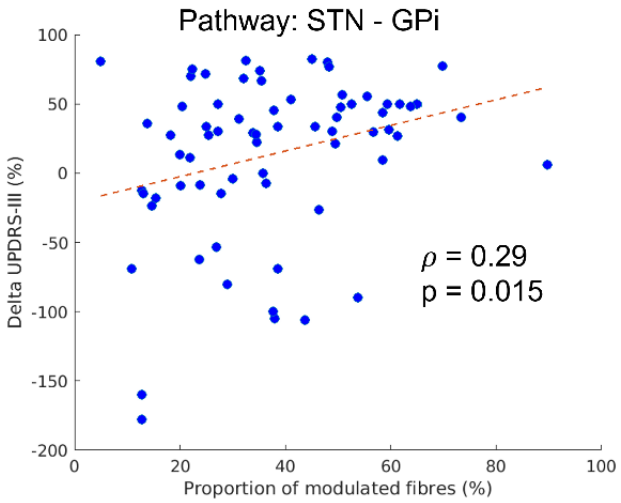

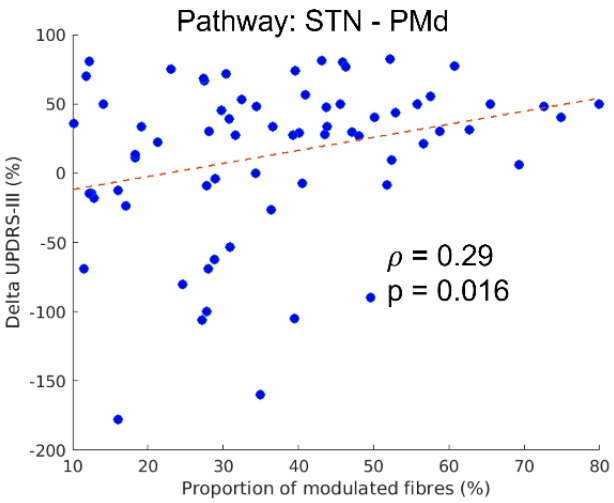

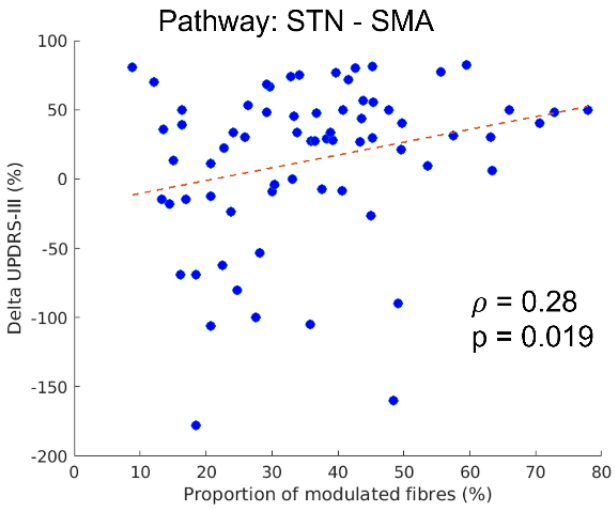

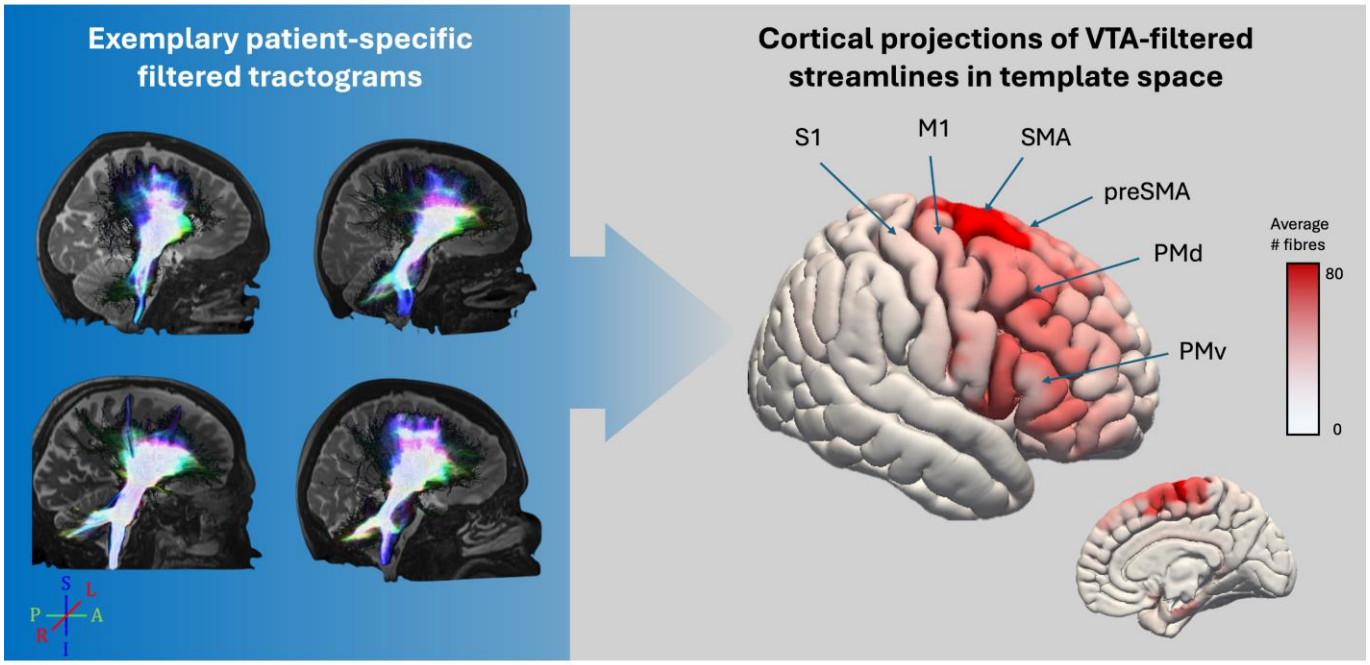

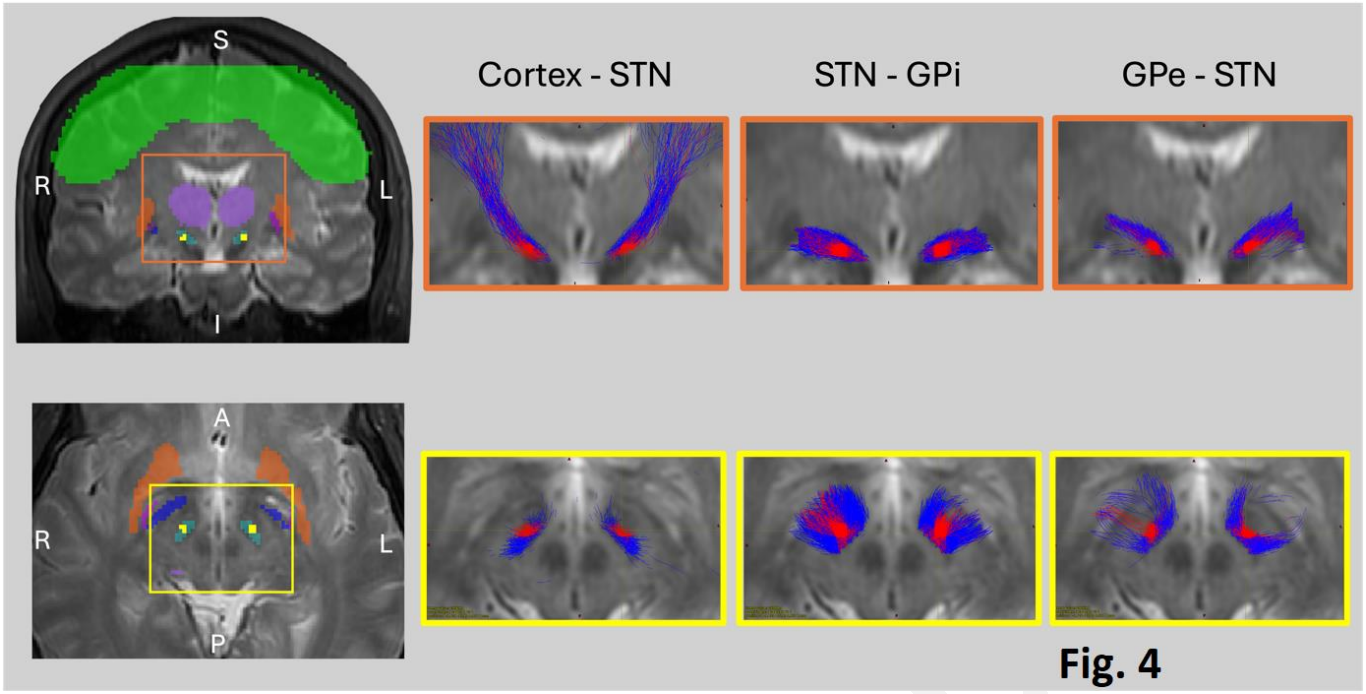

Fig. 4

Table 1 Patient characteristics

Age (years)	63.7 (46.8 – 78.1)		
Sex (female/male)	26/43		
Hoehn-Yahr stage (1/2/3/4)	5/28/25/11		
Duration of disease (years)	10.4 (2.6 – 27.2)		
Volume of tissue activated (µL)	54.0 (2.2 - 305.4)		
Interval (months)	9.0 (2.6 – 20.2)		
	Pre-DBS	Post-DBS	
Levodopa-equivalent daily dose	1096.6 (150 - 2159)	541.5 (0 - 1431)	***
UPDRS-III (Med ON)	21.1 (4 - 43)	16.8 (2 - 47)	**
Tremor	3.4 (0 - 20)	1.5 (0 - 7)	**
Rigidity	6.0 (0 - 17)	3.7 (0 - 14)	***
Bradykinesia	11.8 (0 - 28)	8.3 (0 - 19)	***

Numbers are average (range) or counts. ***p < 0.001; **p < 0.01; *p < 0.05

Table 2 Correlation analysis between proportion of fibres modulated by DBS and percentage change in UPDRS-III score. P-values which survived Benjamini-Hochberg correction are signalled with *

Fibre tract	**Spearman Correlation coefficient**	**P - value**
STN - SMA	0.28	0.019*
STN - preSMA	0.26	0.031*
STN - PMv	0.26	0.034*
STN – PMd	0.29	0.016*
STN – M1	0.21	0.086
STN – S1	0.21	0.088
STN - GPe	0.26	0.031*
STN - GPi	0.29	0.015*

*p<0.05; n.s.: not significant; STN: subthalamic nucleus; SMA: supplementary motor area; pre-SMA: pre-supplementary motor area; PMd/PMv: dorsal/ventral premotor area; M1: primary motor cortex; S1: primary somatosensory cortex; GPe/GPi: external/ internal Globus pallidus

Table 3 Degree of pathway modulation by DBS in good and bad responders with respect to symptom scores. P-values which survived Benjamini-Hochberg correction are signalled with *

	Good response	**Bad response**	**p-value**
Tremor			
STN - SMA	39.8 ± 15.9	31.1 ± 15.0	0.021*
STN - preSMA	42.9 ± 18.1	31.0 ± 16.3	0.006*
STN - PMv	40.4 ± 16.0	31.8 ± 16.8	0.025*
STN – PMd	41.3 ± 16.5	31.6 ± 16.8	0.011*
STN – M1	34.4 ± 14.9	30.2 ± 19.1	0.146
STN – S1	34.8 ± 15.3	31.4 ± 18.9	0.124
STN - GPe	39.6 ± 16.0	30.1 ± 14.7	0.010*
STN - GPi	42.8 ± 17.8	30.5 ± 15.1	0.005*
Rigidity			
STN - SMA	40.6 ± 17.3	29.3 ± 11.0	0.006*
STN - preSMA	42.7 ± 19.7	30.4 ± 13.0	0.009*
STN - PMv	41.7 ± 17.7	29.3 ± 12.2	0.004*
STN – PMd	42.4 ± 18.1	29.3 ± 12.2	0.002*
STN – M1	36.7 ± 17.4	26.4 ± 14.2	0.012*
STN – S1	37.2 ± 17.1	27.7 ± 15.2	0.012*
STN - GPe	40.1 ± 17.4	28.6 ± 10.9	0.005*
STN - GPi	43.5 ± 18.8	28.7 ± 11.3	0.001*
Bradykinesia			
STN - SMA	36.0 ± 14.4	36.0 ± 17.9	0.768
STN - preSMA	37.4 ± 15.6	38.1 ± 21.1	0.796
STN - PMv	36.3 ± 14.7	37.1 ± 19.2	0.966
STN – PMd	36.8 ± 14.9	37.3 ± 19.7	0.861
STN – M1	31.7 ± 14.2	33.6 ± 19.3	0.899
STN – S1	32.2 ± 14.7	34.6 ± 19.3	0.687
STN - GPe	34.4 ± 13.2	36.6 ± 19.0	0.995
STN - GPi	35.8 ± 15.4	39.4 ± 20.1	0.535

Table 4 – Overview of studies using normative connectomes

Study	N	Med.	DBS Test Condition	Follow-up (months)	Outcome	SFG	preMC	PFC	Pre-SMA	SMA	M1	Tha
Horn 2017 [16]*	51 44	Off Off	DBS On vs. Off DBS On vs. pre-op	12-24 6-12	UPDRS-III UPDRS-III	+ +				+ +		
Wang 2021 [17]	33	Off	DBS On vs. pre-op	3-12	UPDRS-III			+	+			
Chen 2022 [18]	98	Off	DBS On vs. pre-op	1	UPDRS-III					+	+	
Strelow 2022 [19]	47	On	DBS On vs. pre-op	6	Freezing of gait		+	+		+	+	
Hacker 2023 [22]	14	On	DBS On vs. pre-op	24	UPDRS-III					+	+	
Gadot 2023 [21]	40	Off	DBS On vs. pre-op	6	UPDRS-III	+				+		+
Fan 2023 [20]	76	On	DBS On vs. pre-op	12	Freezing of gait				+	+		
Hollunder 2024 [23]*	94	On	DBS On vs. Off	12	UPDRS-III					+		
Rajamani 2024 [24]*	237	Off	DBS On vs. Off DBS On vs. pre-op	12-24 6-12	tremor bradykinesia rigidity				 +	 +	+	

*Partially overlapping data sets. SFG: Superior Frontal Gyrus, preMC: pre-Motor Cortex, PFC: Pre-Frontal Cortex, Pre-SMA: pre-Supplementary Motor Area, SMA: Supplementary Motor Area, M1: primary Motor Cortex, Tha: Thalamus

Table 5 – Overview of studies using patient-specific connectomes

Study	N	Med.	DBS Test Condition	F-up (months)	Outcome	SFG	preMC	PFC	Pre-SMA	SMA	M1	Tha	GPi	GPe
Koirala 2016 [43]	15	On/Off	DBS On/Med Off vs. pre-op Med On	n.d.	UPDRS-III					+	+			
Vanegas-Arroyave 2016 [44]	22	Off	DBS On	1	clinical effect	+						+		
Akram 2017 [45]	20	Off	DBS On vs. Off	12	tremor bradykinesia rigidity			 +		 + +	+ 			
Krishna 2019 [47]	24	Off	DBS On vs. pre-op	1	tremor bradykinesia rigidity		+	 + +			+ + 			
Avecillas-Chasin 2019 [46]	13	On	DBS On vs. pre-op	25	UPDRS-III bradykinesia					+ +	+			
Vassal 2020 [48]	9	Off	DBS On vs. pre-op	6	UPDRS-III		+			+	+			
Wang 2021 [17]	33	Off	DBS On vs. pre-op	3-12	UPDRS-III			+	+					
Kahkola 2022 [50]	22	On	DBS On vs. pre-op	12	UPDRS-III unilat.				+					
Gonzalez-Escamilla 2022 [49]	15	Off	DBS On vs. pre-op	3	UPDRS-III					+	+			
Segura-Amil 2023 [51]	20	Off	DBS On	4-6	clinical effect					+	+			
Present study	69	On	DBS On vs pre-op	3-20	UPDRS-III tremor rigidity		+ + +		+ + +	+ + +	 +	 +	+ + +	+ + +

n.d. – not determinable from the manuscript. SFG: Superior Frontal Gyrus, preMC: pre-Motor Cortex, PFC: Pre-Frontal Cortex, Pre-SMA: pre-Supplementary Motor Area, SMA: Supplementary Motor Area, M1: primary Motor Cortex, Tha: Thalamus